ISEIS

Journal of Environmental Informatics 18(1) 38-45 (2011)

Journal of Environmental Informatics

www.iseis.org/jei

Comparison of Six GIS-Based Spatial Interpolation Methods for Estimating Air Temperature in Western Saudi Arabia

K. A. Eldrandaly* and M. S. Abu-Zaid

King Abdulaziz University, Jeddah 21589, Saudi Arabia

Received 20 January 2011; revised 5 July 2011; accepted 18 August 2011; published online 12 September 2011

ABSTRACT. Six GIS-based spatial interpolation methods were compared to determine their suitability for estimating mean monthly air temperature (MMAT) surfaces, from data recorded at nearly 31 meteorological stations representing different climatic conditions in Western Saudi Arabia. The eventual purpose of producing such surfaces is to help making air temperature data be available for a wide variety of scientific uses. The interpolation techniques included four deterministic methods (Inverse Distance Weighted, Global Polynomial, Local Polynomial, and Radial Basis Function (Thin-Plate Spline) and two geostatistical methods (Ordinary Kriging, and Universal Kriging). Quantitative assessment of the continuous surfaces showed that there was a large difference between the accuracy of the six interpolation methods and that the geostatistical methods were superior to deterministic methods. This work also revealed systematic spatial and temporal variations of temperatures in western Saudi Arabia.

Keywords: spatial interpolation, geostatistics, mean monthly temperature, weather stations, Western Saudi Arabia

1. Introduction

Spatial continuous data (surfaces) play a significant role in planning, risk assessment and decision making in environmental management. They are, however, usually not readily available and often difficult and expensive to acquire, especially for mountainous and deep marine regions. As geographic information systems (GIS) and modeling techniques are becoming powerful tools in natural resource management and biological conservation, spatial continuous data of environmental variables are increasingly required. However, spatial data of natural phenomena such as air temperature are often collected from point sources. Therefore, GIS-based spatial interpolation methods are essential for estimating biophysical variables for the unsampled locations (Li and Heap, 2008).

Spatial interpolation is the process of intelligent guesswork, in which the investigator and the GIS attempt to make a reasonable estimate of the value of a continuous field at places where the field has not actually been measured (Longley et al., 2011). Spatial interpolation is more worthwhile if a sufficient density of weather stations is available across the study area. As it is the case in numerous areas of the world, the western portion of Saudi Arabia lacks extensive, elaborate, or evenly distributed network of meteorological stations. With the exception of airport sites, agricultural extensions, and dam facilities, meteorological data are not available for the majority of locations within the study area. Such a shortcoming would necessarily justify interpolation studies for climatic variables, and hence make such viable data available for a wide range of scientific applications.

Selecting an appropriate GIS-spatial interpolation method is a key success factor of surface analysis since different methods of interpolation can result in different surfaces and ultimately different results .Among numerous interpolation methods, no method is uniquely optimal, and so the best interpolation method for a specific situation can only be obtained by comparing their results. For example, Luo et al. (2008) compared seven spatial interpolation techniques (Trend Surface Analysis, Inverse Distance Weighting, Local Polynomial, Thin Plate Spline, Kriging and Cokriging) to determine their suitability for estimating daily mean wind speed surfaces, from data recorded at nearly 190 locations across England and Wales. Cross – validation was used to evaluate the performance of each interpolation method by calculating the root mean square error (RMSE) for each interpolation method. The results indicated that Cokriging was most likely to produce the best estimation of continuous surface for wind speed in the study area. Sun et. al. (2009) compared three interpolation methods (Inverse Distance Weighting, Radial Basis Function, and Kriging) to determine their suitability for interpolating depth to groundwater in the Minqin oasis of northwest China. Root mean square error (RMSE) was used to evaluate the performance of each interpolation method. Results of this study indicated that simple Kriging was the optimal method for interpolating depth to groundwater in the study area.

* Corresponding author. Tel.: +966 507588510; fax: +966 2 6404043.
E-mail address: keldrandaly@kau.edu.sa (K. A. Eldrandaly).

ISSN: 1726-2135 print/1684-8799 online
 doi:10.3808/jei.201100197

While there have been comparisons of interpolation methods for temperature and precipitation in numerous areas of the world, (see for example, Holdaway, 1996; Dodson and Marks, 1997; Thornton et al., 1997; Bolstad et al., 1998; Couralt and Monestiez, 1999; Xia et al., 1999; Hartkamp et al., 1999; Shen et al., 2001; Xia et al., 2001; Jarvis and Stuart, 2001; Kastelec and Kosmelj, 2002; Hasenauer et al., 2003; Garen and Marks, 2005; Stahl et al., 2006; Attorre et al., 2007; Hofstra et al., 2008), review of the literature reveals that no interpolation study of climatic variables has been applied to the study area (western Saudi Arabia). However, there is a single attempt to introduce a method for estimating mean monthly air temperatures in western Saudi Arabia (Al-Jerash, 1983).

In this study Six GIS-based spatial interpolation methods were compared to determine their suitability for estimating mean monthly air temperature surfaces, from data recorded at nearly 31 meteorological stations representing different climatic conditions in Western Saudi Arabia. The cross-validation method is used to assess which method gives the best interpolation. Then, the best method was used to analyze temporal and spatial variations of mean monthly temperature.

2. Materials and Methods

2.1. Study Area

The western portion of Saudi Arabia covers a considerable area of the country, about 382,000 Square Kilometers. It extends in the north – south direction for sixteen degrees of latitude (16 ~ 32 North) along the Red Sea coast. In the east-west direction, it spans from the coast to the high mountain range of Sarawat as shown in Figure 1. Delineation of Western Saudi Arabia has been geographically adopted by many authors (Al-Jerash, 1983; Al-Mowalad, 1983; Habib, 1989; Al-Harbi, 2009).

Topographically, the study area comprises a variety of sub-regions as shown in Figure 1. They include: (1) Tihama, a narrow, low-lying, gradually sloping, coastal plain, (2) the western highlands of the Sarawat mountains which extend parallel to the Red Sea coast, and (3) a group of elevated plateaus. Elevation in the area ranges between sea level to more than 3000 meters at the summits of Asir region to the south.

The Red Sea coastal plain varies in width on a north-south direction. While it extends for about 45 km from the coast near Jazan in the south, it gradually narrows to about 20 km to the north (Sagga, 1995). Furthermore, the plain becomes extremely narrow in the northernmost parts where the coast nearly meets the foothills (Saif, 2000).

The western highlands extend from east to west for between 120 ~ 200 kilometers, with an overall altitude of 900 meters (Al-Mowalad, 1983). Elevation above sea level gradually increases towards the south exceeding 3000 meters in the southernmost parts of the study area. Elevation of the interior plateaus ranges between 800 ~ 1500 meters. The mountain range gently slopes to the east, while rough slopes are found on the west.

Climatic conditions in the study area are generally influenced by such factors as; latitude, geographical location, dominant pressure conditions, and topography. As far as air temperatures, the study area is generally characterized with conditions typical of arid and semi-arid regions of the world. Air temperatures tend to vary widely in both spatial as well as temporal levels. However, temperature tends to increase in a southerly direction all year round, on one hand, and decreases with altitude on the other. For example mean January temperatures ranges between 9 ~ 11 degrees at Al-Namas (2600 meters), and Tabouk (28, 22 N) respectively. The mean for the same month exceeds 25 degrees at Jazan, Sabya, and Malaki in the extreme south of the study area. On the other hand, July mean temperature ranges between 20 ~ 23 degrees in high altitude stations such as Al-Namas, Abha, and Khamis Mushait at 2600, 2200 and 2057 meters respectively. At the lowlands and on the coast (north and south), it is not uncommon for the mean in this month to exceed 30 degrees (Jeddah, Jazan, Sabya, Tabouk, and Najran), until it reaches the upper thirties in the interior portions as in Madinah for example.

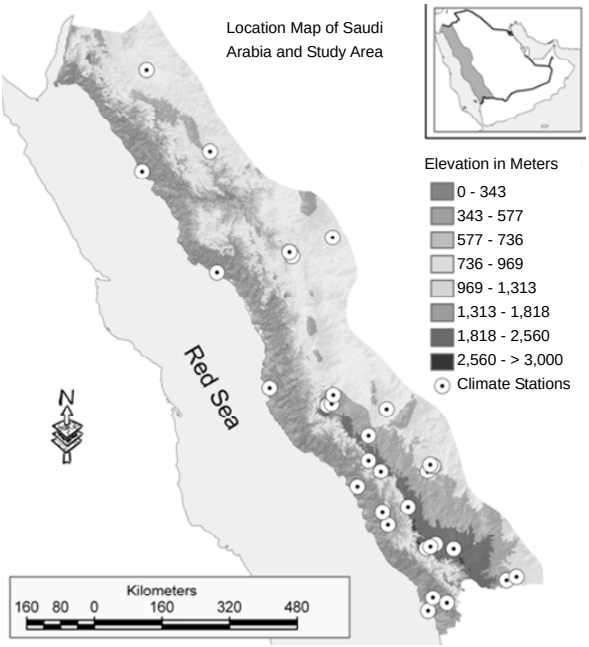

Figure 1. Study Area and Climate Stations.

2.2. Data Collection

The data used in this study comprise continuous records of mean monthly air temperature for the period (1970 ~ 1986) in 31 stations scattered throughout the study area as shown in Figure 1. Air temperatures, along with other meteorological elements, are regularly recorded at airport sites, ten of which are found in the study area. Observations are also made at agricultural extensions and dam sites. These data have been originally provided in part by the Meteorology Section of the presidency of Meteorology and Environmental Protection, and in part by the Hydrology Division of the Ministry of Agriculture and Water. However, and despite the small number of

stations in the study area, the distribution of measurement locations would permit: (1) Representation of the variant physical regions in the study area, and thus the inclusion of a wide range of different altitudes (between sea level and more than 2600 meters), and (2) Taking into account latitudinal and longitudinal differences in the assessment of their influence on the performance and accuracy of interpolation methods subjected to comparison in this study.

2.3. Interpolation Methods

The interpolation methods used in this study were performed by ESRI ArcGIS® Geostatistical Analyst 9.3. Geostatistical Analyst is an extension to the ArcGIS Desktop that provides a powerful suite of tools for spatial data exploration and surface generation using sophisticated statistical methods. Geostatistical Analyst provides two groups of interpolation techniques: deterministic and geostatistical. All methods rely on the similarity of nearby sample points to create the surface. Deterministic techniques use mathematical functions for interpolation. Geostatistics relies on both statistical and mathematical methods, which can be used to create surfaces and assess the uncertainty of the predictions. This section briefly introduces the different interpolation methods used in this study, detailed descriptions of these methods are reported elsewhere (ESRI, 2001; Li and Heap, 2008; Chang, 2010; Lloyd, 2010).

2.3.1. Deterministic Methods

Deterministic interpolation methods create surfaces from measured points, based on either the extent of similarity (e.g. Inverse Distance Weighted) or the degree of smoothing (e.g. Radial Basis Functions). Deterministic interpolation methods can be divided into two groups: global and local. Global methods calculate predictions using the entire dataset. Local methods calculate predictions from the measured points within neighborhoods, which are smaller spatial areas within the larger study area. Geostatistical Analyst provides the Global Polynomial as a global interpolator and the Inverse Distance Weighted, Local Polynomial, and Radial Basis Functions as local interpolators. Deterministic interpolation techniques may be exact or inexact interpolators. Exact interpolators such as Inverse Distance Weighted Interpolation and Radial Basis Functions generate a surface that passes through the control points. In contrast, inexact interpolators such as Global and Local Polynomial predict a value at the point location that differs from its known value.

A-Inverse Distance Weighted (IDW) Interpolation

IDW is the workhorse of spatial interpolation, the method that is most often used by GIS analysts. It employs the Tobler's First Law of Geography by estimating unknown measurements as weighted averages over the known measurements at nearby points, giving the greatest weight to the nearest points (Longley et al., 2011). The general equation for IDW method is shown in equation (1):

$$z_0 = \frac{\sum_{i=1}^{n} z_i \frac{1}{d_i^k}}{\sum_{i=1}^{n} \frac{1}{d_i^k}} \quad (1)$$

Where z_0 is the estimated value at point *0*, z_i is the z value at known point i, d_i is the distance between point i and point *0*, n is the number of known points used in estimation, and k is the specified power which controls the degree of local influence (Chang, 2010).

B-Global Polynomial (GP) Interpolation

GP interpolation simply uses multiple regression methods on all of the data. A response or trend surface is fitted to the x-and y-coordinates, which are the covariates. A first-order Global Polynomial (linear) fits a single plane through the data as shown in equation (2):

$$z(x_i, y_i) = \beta_0 + \beta_1 x_i + \beta_2 y_i + \varepsilon(x_i, y_i) \quad (2)$$

where $z(x_i, y_i)$ is the datum at location (x_i, y_i), β_i are parameters, and $\varepsilon(x_i, y_i)$ is a random error. A second-order Global Polynomial (quadratic) fits a surface with a bend in it, allowing surfaces representing valleys; a third-order Global Polynomial (cubic) allows for two bends; and so forth, up to a 10 are allowed in Geostatistical Analyst (ESRI, 2001).

C-Local Polynomial (LP) Interpolation

As with global polynomials a least square polynomial fit to the data is applied, with options for Order 1, 2 or 3 equations. However, instead of fitting the polynomial to the entire dataset it is fitted to a local subset defined by a window. The size of this window needs to be large enough for a reasonable number of data points to be included in the process. One further adjustment is made to this procedure — a measure of distance-based weighting is included, so the least squares model is in fact a weighted least squares fit. The weights are computed using a power function of distance as a fraction of the window size. The simplest case is where the moving window is a circle with radius R. If the distance between grid point (x_i, y_i) and a data point (x, y) within the circle is denoted d_i, then the weight w_i is given by equation (3) and the least squares procedure then involves minimizing the expression given by equation (4) (De Smith et. al., 2011):

$$w_i = (1 - \frac{d_i}{R})^p \quad (3)$$

$$\sum_{i=1}^{n} w_i (f(x_i, y_i) - z_i)^2 \quad (4)$$

where p is a user definable power and If p=0 all the weights are 1.

D-Radial Basis Functions (RBF) Interpolation

RBF methods are a series of exact interpolation algorithms that a surface must go through in each measured sample location. Geostatistical Analyst includes five different RBF methods: Thin-Plate Spline, Spline with Tension, Completely Regularized Spline, Multiquadric Function, and Inverse Multiquadric Function. Each basis function has a different shape and results in a slightly different interpolation surface. In this paper, Thin-Plate Spline (TPS) was used. TPS creates a surface that passes through the control points with a minimum curvature surface. The approximation of TPS is calculated as shown in equation (5):

$$Q(x,y) = f_i = \sum_{i=1}^{n} A_i d_i^2 \log d_i + a + bx + cy \quad (5)$$

Where x and y are the x-, y-coordinates of the point to be interpolated, $d_i^2 = (x - x_i)^2 + (y - y_i)^2$, x_i and y_i are the x-, y-coordinates of the control point i, n is the number of control points, and f_i is the known value at control point i. Thin –plate spline consists of two components: *(a + bx + cy)* represents the local trend function, and $d_i^2 \log d_i$ represents minimum curvature surface basis function. The coefficients A_i, *a, b,* and *c* are determined using a linear system of equations (Chang, 2010).

2.3.2. Geostatistical Methods

Geostatistical interpolation methods create surfaces incorporating the statistical properties of the measured data. These techniques produce not only prediction surfaces but also error or uncertainty surfaces, giving the analyst an indication of how good the predictions are. Many methods are associated with geostatistics, but all are in the Kriging family. Originated in mining and geologic engineering in the 1950s, Kriging has since been adopted in a wide variety of disciplines. Kriging assumes that the spatial variation of an attribute is neither totally random (stochastic) nor deterministic. Instead, the spatial variation may consist of three components: a spatially correlated component, representing the variation of the regionalized variable; a "drift" or structure, representing a trend; and a random error term. The interpretation of these components has led to development of different Kriging methods for spatial interpolation. Ordinary, Simple, Universal, Probability, Indicator, and Disjunctive Kriging are available in the Geostatistical Analyst. In this study, Ordinary and Universal Kriging were used.

A-Ordinary Kriging

Assuming the absence of a drift, Ordinary Kriging (OK) focuses on the spatially correlated component and uses the fitted semivariogram, a diagram relating the semivariance to the distance between sample points used in Kriging, directly for interpolation. The estimator of ordinary Kriging is given by equation (6):

$$z^*(x_0) = \sum_{i=1}^{n} \lambda_i z(x_i) \quad (6)$$

Where $z^*(x_0)$ is the estimate value at x_0, $z(x_i)$ is the measure value at the x_i and λ_i is the weight assigned for the residual of $z(x_i)$ (Sun et al., 2009).

B-Universal Kriging

Universal Kriging (UK) assumes that the spatial variation in z values has a drift or a trend in addition to the spatial correlation between the sample points. By definition of the drift component, the expected value $m(x)$ of $z(x)$ at point z is given by equation (7) and the estimator of universal Kriging is given by equation (8) (Sun et al., 2009):

$$E[z(x)] = m(x) \quad (7)$$

$$z^*(x_0) = \sum_{i=1}^{n} \lambda_a z_a \quad (8)$$

where $n$the number of is available sampling data, $z^*(x_0)$ is the estimate value, z_a is the measured value at sampling point $a(a = 1,....,n)$, and λ_a is the weighting coefficient, which is calculated with unbiased and minimum error variance.

2.4. Assessment of Interpolation Outputs

Cross-Validation was used to evaluate the performance of each interpolation method. It is one of the most commonly used statistical techniques for comparing interpolation methods. Cross-Validation compares the interpolation methods by repeating the following procedure for each interpolation method to be compared (Chang, 2010): (1) Remove a known point from the data set, (2) Use the remaining points to estimate the value at the point previously removed, and (3) Calculate the predicted error of the estimation by comparing the estimated with the known value. After completing the procedure for each known point, two common diagnostic statistics, Root Mean Square Error (RMSE) and the standardized RMSE, are calculated to assess the accuracy of the interpolation method as shown in equations (9) and (10):

$$RMSE = \sqrt{\frac{1}{n}\sum_{i=1}^{n}\left(z_i - z\right)^2} \quad (9)$$

$$\text{Standardized } RMSE = \frac{RMSE}{S} \quad (10)$$

where z_i and z are the measured and the estimated value at the sampling point $i\,(i = 1,2,...n)$; n is the number of values used for the estimation; and S is the standard error.

The RMSE statistic is available for all exact local me-

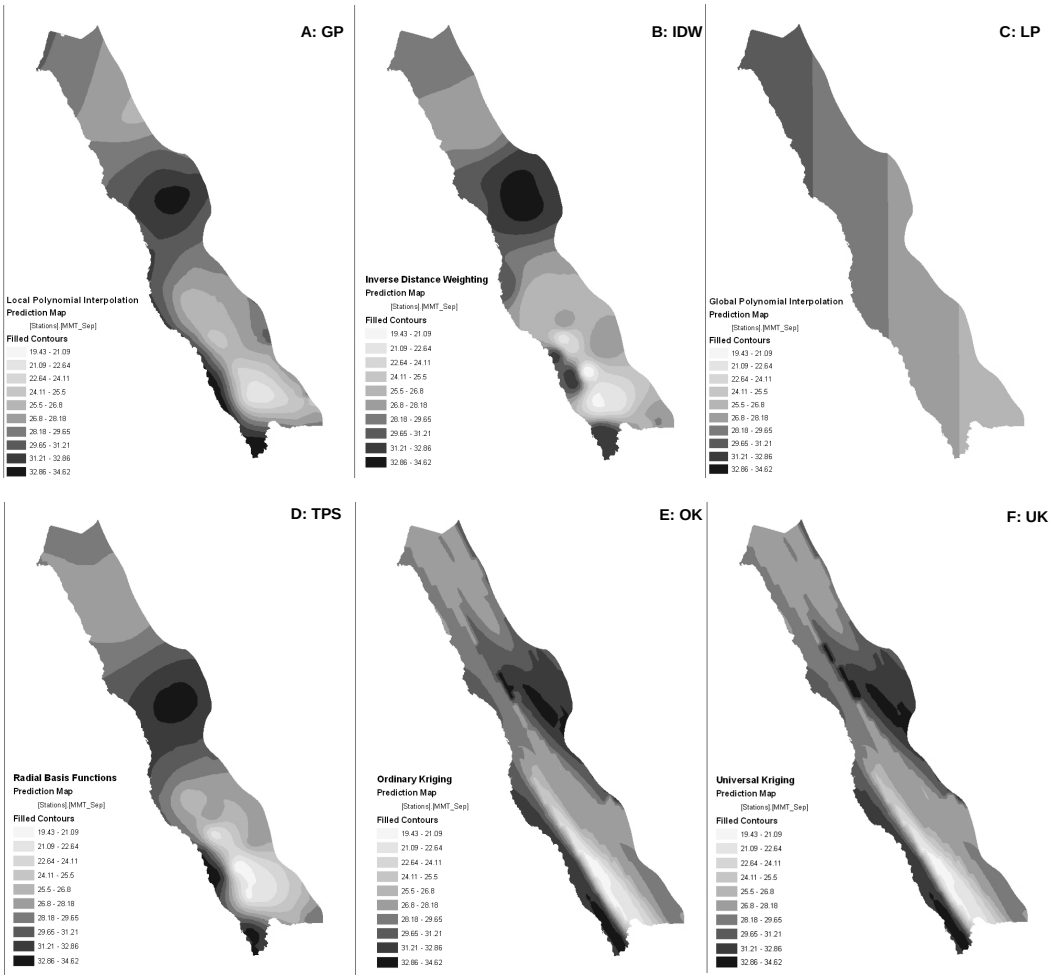

Figure 2. Interpolation of September mean monthly temperature (MMAT) using 6 different methods.

thods, but the Standardized RMSE is only available for Kriging because the variance is required for computation. A better interpolation method should yield a smaller RMSE and a better Kriging method should yield a smaller RMSE and a Standardized RMSE closer to 1 (Chang, 2010).

3. Results and Discussion

3.1. Comparison of Interpolation Methods

Mean Monthly Air Temperature for four selected months (January, March, July, September) as representatives of the four temperate seasons (Winter, Spring, Summer, Autumn) in Western Saudi Arabia was interpolated in turn using six GIS-based interpolation techniques (IDW, LP, GP, TPS, OK, UK). Figure 2 shows samples of interpolated surfaces using different methods. RMSE (for the six methods) and Standardized RMSE (for only OK and UK) were then calculated using Cross-Validation as shown in Table 1. Figure 3 shows a sample of cross validation comparison between two methods. The minimal RMSE are obtained by OK and UK, which have almost the same RMSE and Standardized RMSE for all months. Thus those two methods are the optimal methods for interpolating mean monthly temperature in the study area.

3.2. Temporal and Spatial Variation of Mean Monthly Temperature in Western Saudi Arabia

The temporal and spatial variations of mean monthly air temperature (MMAT) in Western Saudi Arabia were interpolated using the Universal Kriging method (UK). The following two Sections briefly describe these variations.

3.2.1. Spatial Distribution of Air Temperatures in Western Saudi Arabia

Figure 4 shows four maps of interpolated mean monthly air temperature (MMAT) in the study area for January, March, July, and September which are, in the same time, representatives of winter, spring, summer, and autumn respectively. Inspection of these maps clearly indicates a zonal distribution of interpolated (MMAT) that is largely influenced by such factors as longitude, latitude, and altitude. In general, air temperatures are higher along the coastal zone as well as throughout the interior parts of relatively lower elevations in the study area. This situation is dominant in the area all year round, keeping in mind a wide range of differences between seasons (these temporal variations are discussed in the following section). On the other hand, areas with higher altitudes

Table 1. RMSE for the Different Methods

Month	RMSE						Standardized RMSE	
	IDW	LP	GP	TPS	OK	UK	OK	UK
Jan	3.773	3.283	4.598	2.956	1.700	1.700	0.6189	0.6189
Mar	3.278	3.283	4.618	2.975	1.751	1.751	0.5076	0.5076
Jul	2.798	3.328	4.708	2.745	1.859	1.859	0.5787	0.5787
Sep	2.743	3.227	4.682	2.593	1.614	1.612	0.5405	0.5303

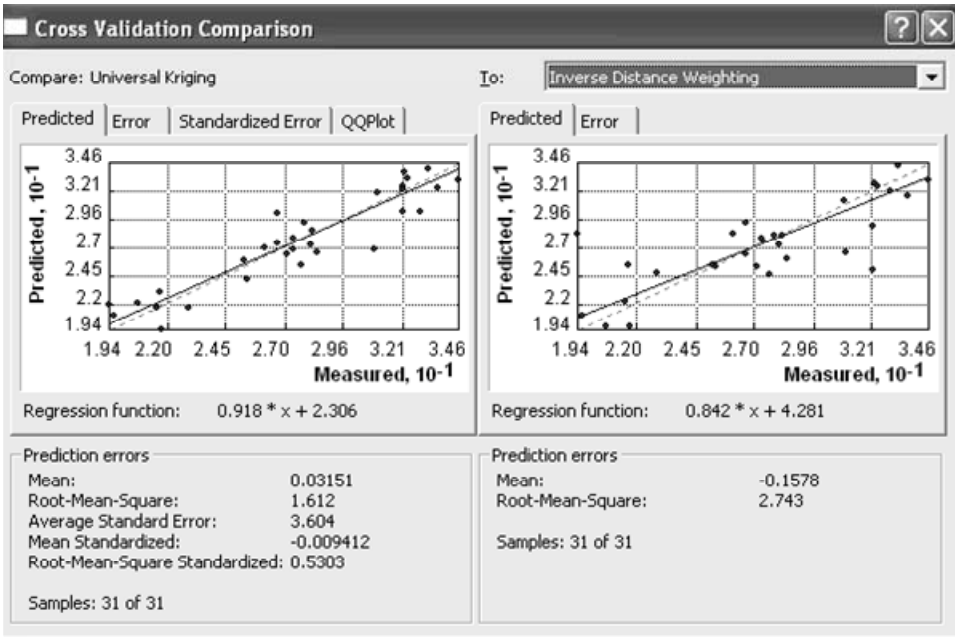

Figure 3. A sample of cross validation comparison.

especially mountainous portions in the south interpolation results showed general decrease in temperature throughout the year. However, the magnitude of such a reduced tendency varies with both time of the year, and altitude above sea level (Figure 4).

Interpolated air temperature for interior, relatively lower portions of the study area greatly differs with seasons. During the hot times of the year these areas come among the hottest locations throughout Saudi Arabia (Figure 4C and 4D). During In winter, on the other hand, these areas reflect extremely cold conditions, and come among the coldest spots, for this time of the year, especially in the far north of the study area (Figure 4A).

In addition to the aforementioned factors, the interior southernmost portions of the study area, spatial aspects of interpolated MMAT appear to have been greatly influenced by its position regarding the growth and retreat of subsequent weather systems experienced throughout the march of seasons. During the colder part of the year (late autumn – late spring), the area is under the influence of weather systems coming from the north (the Mediterranean Region). For the warmer periods, the area is under the influence of weather effects of southern origin (monsoon systems). In all cases, the effects are reflected in lower air temperatures (Figure 4).

3.2.2. Temporal Distribution of Air Temperatures in Western Saudi Arabia

Results indicate widespread and distinctive patterns of differences and variations regarding interpolated monthly mean air temperature (MMAT) in the study area. These differences and variations relate to such characteristic as the magnitude as well as the distribution of interpolated variable. Interpolated values for winter (January) range between 10.06 and 26.29 degrees centigrade, while summer (July) values were as high as between 20.51 and 35.34 degrees (Figures 4A and 4C). Furthermore, the spatial distribution of interpolated MMAT differed widely among seasons. For winter, the lowest temperatures are found in the interior of the northernmost portion in the study area, followed by sections of the high mountainous region in the south. Higher values are spread throughout most of western Saudi Arabia including coastal and interior, both in the north and south of the study area. The highest temperatures are typically distributed throughout the southern half of the coastal plain and its neighboring low-lying interior segments. This pattern of the spatial distribution of interpolated MMAT comes in agreement with that important role of such variables as longitude, latitude, and elevation above sea level.

As for summer, interpolated values show different arrangements and spatial patterns (Figure 4C). The lowest values

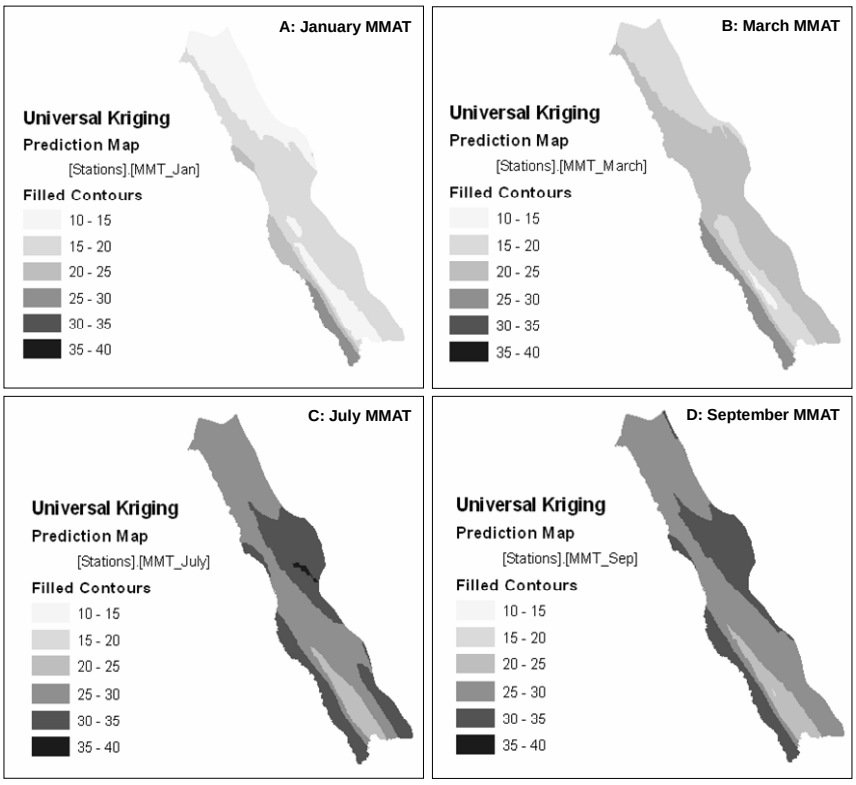

Figure 4. Spatial and Temporal Variation of mean monthly temperature (MMAT).

are restricted to areas of high elevations especially the mountainous region of southwestern Saudi Arabia and to a lesser degree within the surrounding plateaus to the north and east of such region. Higher temperatures are distributed throughout most of the northern half of the study area including both coastal and interior segments. Like in winter, the southern half of the coastal plain still experiences high levels of air temperatures in the summer. The highest temperatures are found in the interior, moderately elevated plains within the northern half of the study area.

4. Conclusions

Ordinary Kriging and Universal Kriging are the most optimal methods for interpolating mean monthly air temperature in this region. This conclusion is based on available air temperature data recorded at nearly 31 meteorological stations representing different climatic conditions in Western Saudi Arabia during the period (1970 ~ 1986), which were in turn interpolated using six GIS-based interpolation methods. Cross-Validation was used to compare the various interpolation methods. Diagnostic Statistic indicated that Ordinary and Universal Kriging had the smallest RMSE and thus they are considered the optimal methods for interpolating air temperature in this region.

Results have shown a zonal pattern of interpolated air temperatures that is largely influenced by such factors as longitude, latitude, and altitude. In general, air temperatures are higher along the coastal zone as well as throughout the interior parts of relatively lower elevations in the study area.

Results have also revealed widespread and distinctive patterns of differences and variations regarding the magnitude as well as the distribution of interpolated monthly mean air temperature in the study area. The spatial distribution of interpolated mean monthly air temperature differed widely among seasons.

These patterns of spatial as well as temporal distributions of interpolated mean monthly air temperatures comes in agreement with that important role of such variables as longitude, latitude, and elevation above sea level.

Acknowledgments. This research was supported by the Research Grants Program of King Abdulaziz University, Jeddah, Saudi Arabia.

References

Al-Harbi, S.A. (2009). Rainfall Characteristics over Western Saudi Arabia, *M.Sc. Thesis*, College of Arts and Humanities, King Abdulaziz University, Jeddah, Saudi Arabia.

Al-Jerash, M.A. (1983). Models for Estimating Average Annual Rainfall over the West of Saudi Arabia, *J. Fac. Arts Humanities*, 3, 107-150.

Al-Mowalad, F.M. (1983). The Climate of Western Saudi Arabia, *M.Sc. Thesis*, College of Arts, King Saud University, Riyadh, Saudi Arabia.

Attorre, F., Marko, A., De Sanctis, M., Francesconi F., and Bruno, F. (2007). Comparison of interpolation methods for mapping climatic and bioclimatic variables at regional scale, *Int. J. Climatol.*, 27(13), 1825-1843. http://dx.doi.org/10.1002/joc.1495

Bolstad, P.V., Swift, L., Collins, F., and Regniere, J. (1998). Measured and predicted air temperatures at basin to regional scales in

the southern Appalachian mountains, *Agric. For. Meteorol.*, 91, 161-178. http://dx.doi.org/10.1016/S0168-1923(98)00076-8

Chang, K. (2010). *Introduction to Geographic Information Systems*, McGraw-Hill, New York.

Couralt, D., and Monestiez, P. (1999). Spatial interpolation of air temperature according to atmospheric circulation patterns in southeast France, *Int. J. Climatol.*, 19, 365-378. http://dx.doi.org/10.1002/(SICI)1097-0088(19990330)19:4<365::AID-JOC369>3.0.CO;2-E

Dodson, R., and Marks, D. (1997). Daily air temperature interpolated at high spatial resolution over a large mountainous region, *Clim. Res.*, 8, 1-20. http://dx.doi.org/10.3354/cr008001

De Smith, M., Longley, P., and Goodchild, M., (2011). Geospatial Analysis- A Comprehensive guide to principles, techniques, and software tools. http://www.spatialanalysisonline.com/output/(acessed June, 2011).

ESRI (2001). *Using ArcGIS Geostatistical Analyst*, ESRI Press, Redlands.

Garen, D.C., and Marks, D. (2005). Spatially distributed energy balance snowmelt modeling in a mountainous river basin: estimation of meteorological inputs and verification of model results, *J. Hydrol.*, 315, 126-153. http://dx.doi.org/10.1016/j.jhydrol.2005.03.026

Habib, B.O. (1989). Effective Rainfall in western Saudi Arabia-A study in Applied Climatology, *M.Sc. Thesis*, Jeddah Girls College, Jeddah, Saudi Arabia.

Hartkamp, A.D., De Beurs, K., Stein, A., and White, J.W. (1999). *Interpolation Techniques for Climate Variables*, MRG-GIS Series 99-01, Mexico, D.F.: CIMMYT.

Hasenauer, H., Merganicova, K., Petritsch, R., Pietsch, S.A., and Thornton, P.E. (2003). Validation of daily climate interpolations over complex terrain in Austria, *Agric. For. Meteorol.*, 119, 87-107. http://dx.doi.org/10.1016/S0168-1923(03)00114-X

Hofstra, N., Malcolm, H., Mark, N., Phil, J., and Christoph, F. (2008). Comparison of six methods for the interpolation of daily European climate data, *J. Geophys. Res. (D Atmos.)*, 113, no. D21: D2111 0.1- D21110.19.

Holdaway, M.R. (1996). Spatial modeling and interpolation of monthly temperature using kriging, *Clim. Res.*, 6, 215-225. http:// dx.doi.org/10.3354/cr006215

Jarvis, C.H., and Stuart, N. (2001). A comparison among strategies for interpolating maximum and minimum daily air temperatures. Part II: the interaction between number of guiding variables and the type of interpolation method, J. Appl. Meteorol., 40, 1075-1084.http://dx.doi.org/10.1175/1520-0450(2001)040<1075:ACASFI>2.0.CO;2

Kastelec, D., and Katarina, K. (2002). *Spatial interpolation of mean yearly precipitation using universal Kriging*, in: Andrej, M., Anuska, F., (Eds.), Development in Statistics, Zvezki, M., 17, Ljubljana: FDV.

Li, J., and Heap, A.D. (2008). *A Review of Spatial Interpolation Methods for Environmental Scientists*, Geoscience Australia, Record 2008/23.

Lloyd, C. (2010). *Spatial Data Analysis: An Introduction for GIS Users*, Oxford University Press.

Longley, P., Goodchild, M., Maguire, D., and Rhind, D. (2011). *Geographic Information Systems and Science*, Wiley, New York.

Luo, W., Taylor, M., and Paker, S., (2008). A comparison of spatial interoplation methods to estimate continous wind speed surfaces using irregularly distributed data from England and Wales, *Int. J. Climatol.*, 28, 947-959. http://dx.doi.org/10.1002/joc.1583

Sagga, A.M.S. (1995). *The Physical Geography of Saudi Arabia*, Dar Zahran, Jeddah, Saudi Arabia.

Saif, M.M. (1998). *Geography of Saudi Arabia*, Dar Al-Maarifah, Cairo, Egypt.

Shen, S., Samuel, P., Dzikowski, P., Guilong, L., and Griffith, D. (2001). Interpolation of 1961-1997 daily temperature and precipitation data onto Alberta polygons of ecodistrict and soil landscapes of Canada, *J. Appl. Meteorol.*, 12, 2162-2177. http://dx. doi.org/10.1175/1520-0450(2001)040<2162:IODTAP>2.0.CO;2

Stahl, K., Moore, R.D., Floyer, J.A., Asplin, M.G., and McKendry, I.G. (2006). Comparison of approaches for spatial interpolation of daily air temperature in a large region with complex topography and highly variable station density, *Agric. For. Meteorol.*, 139, 224-236. http://dx.doi.org/10.1016/j.agrformet.2006.07.004

Sun, Y., Kang, S., Li, F., and Zhang, L. (2009). Comparison of interpolation methods for depth to groundwater and its temporal and spatial variations in the Minqin oasis of northwest China, *Environ. Model. Software*, 24, 1163-1170. http://dx.doi.org/10.1016/j.envsoft.2009.03.009

Thornton, P.E., Running, S.W., and White, M.A. (1997). Generating surfaces of daily meteorological variables over large regions of complex terrain, *J. Hydrol.*, 190, 214-251. http://dx.doi.org/10.1016/S0022-1694(96)03128-9

Xia, Y., Fabian, P., Winterhalter, M., and Zhao, M. (2001). Forest climatology: estimation and use of daily climatological data for Bavaria, Germany, *Agric. For. Meteorol.*, 106, 87-103. http://dx.doi.org/10.1016/S0168-1923(00)00210-0

Xia, Y., Winterhalter, M., and Fabian, P. (1999). A model to interpolate monthly mean climatological data at Bavarian forest climate stations, *Theor. Appl. Climatol.*, 64(1-2), 27-38. http://dx.doi.org/10.1007/s007040050108